Phytoplankton size structure and primary production in a highly dynamic coastal ecosystem (Ría de Vigo, NW-Spain): Seasonal and short-time scale variability

Pedro Cermeño [a,*], Emilio Marañón [a,b], Valesca Pérez [a], Pablo Serret [a], Emilio Fernández [a], Carmen G. Castro [c]

[a] *Departamento de Ecología y Biología Animal, Facultad de Ciencias del Mar, Universidad de Vigo, 36310 Vigo, Spain*
[b] *Laboratoire d'Océanographie de Villefranche, CNRS-UPMC, 06234 Villefranche-sur-Mer, France*
[c] *Instituto de Investigaciones Marinas, CSIC, Eduardo Cabello 6, 36208 Vigo, Spain*

Abstract

Size-fractionated phytoplankton biomass and primary production, together with net community metabolism, were measured in a coastal ecosystem (Ría de Vigo, NW-Spain) during a full annual cycle (July 2001–July 2002). On a seasonal scale, this ecosystem was characterized by two distinct oceanographic conditions, namely upwelling and downwelling favourable seasons. During the upwelling season, total chlorophyll a (Chl a) and particulate organic carbon production rates (POC-pr) were in the range 36–129 mg Chl a m^{-2} and 89–834 mg C m^{-2} h^{-1}, respectively, and were mainly accounted for (>80%) by the microphytoplankton size fraction (>20 μm). During the downwelling season, total Chl a and POC-pr were much lower (<27 mg Chl a m^{-2} and <97 mg C m^{-2} h^{-1}, respectively), and the pico- (<2 μm) and nano- (2–20 μm) phytoplankton size fractions significantly increased their contribution to total Chl a (46–87%) and POC-pr (30–86%). The seasonal and short-time scale variability in the hydrographic conditions, in particular upwelling intermittency, provides a feasible explanation for the continuous dominance of large-sized phytoplankton during the upwelling period. Shelf water intrusions, continuous vertical mixing and the size-dependent limitation in light acquisition (package effect), suffered in a higher degree by larger phytoplankton, were likely to account for the shift in phytoplankton size structure during the downwelling period. During the upwelling season, community respiration represented a minor fraction of gross primary production (15–30%), which highlights the large export potential of organic matter by this ecosystem. On the contrary, community respiration accounted for a major fraction of primary production (85%) during the downwelling period, which suggests that most of the photosynthesised organic matter was remineralised within the ecosystem. Although the microbial plankton community of the Ría de Vigo exhibits a net autotrophic functioning throughout the year, the magnitude of the carbon flows and budgets seems to be dependent on phytoplankton size structure.
© 2005 Elsevier Ltd. All rights reserved.

Keywords: phytoplankton; size structure; primary production; hydrodynamics; coastal waters; Ría de Vigo

1. Introduction

Phytoplankton size structure plays a central role in controlling the fate of biogenic carbon (C) in pelagic ecosystems (Legendre and Le Fèvre, 1989; Legendre and Rassoulzadegan, 1996). Typically, communities dominated by large-sized phytoplankton have a large potential to export organic matter to upper trophic levels, through a short, classical food chain, and to adjacent systems. By contrast, communities dominated by small-sized phytoplankton are characterized mainly by complex microbial food webs that favour the recycling of organic matter within the euphotic layer. Many studies have confirmed the persistence, in terms of biomass and productivity, of small-sized phytoplankton, which can be regarded as a background component of the planktonic community. However, their relative contribution at the community level is highly variable,

---

* Corresponding author.
E-mail address: pca@uvigo.es (P. Cermeño).

depending on the dynamics of large-sized phytoplankton (Raimbault et al., 1988; Chisholm, 1992). In order to explain this, some authors have pointed out that stability–unstability conditions in the water column play a major role in controlling phytoplankton size structure. On one hand, hydrodynamical forcing controls nutrient supply to the euphotic layer. High nutrient concentrations cause a preferential increase in the biomass and primary production of larger phytoplankton (Chisholm, 1992; Agawin et al., 2000). On the other hand, water column stability determines the size-differential residence time of phytoplankton cells within the euphotic layer, either favouring large-sized phytoplankton losses by passive sinking or accumulating them through the effect of vertical motion (Margalef, 1978; Malone, 1980; Rodríguez et al., 2001). In addition to these mechanisms, zooplankton grazing is also important in controlling the size distribution of phytoplankton communities (Banse, 1992; Kiørboe, 1993). While biomass and production of small phytoplankton are controlled strictly by microzooplankton grazing, large phytoplankton and their grazers may often be uncoupled in time, on account of the longer generation times of mesozooplankton. As a result, phytoplankton size structure depends on a variety of factors, which ultimately are controlled by hydrodynamics of the system (Riegman et al., 1993).

Net community production, defined as the difference between gross primary production and community respiration, provides an overall insight into the biogeochemical functioning of pelagic ecosystems. Highly productive ecosystems, such as those influenced by upwelling, typically exhibit a net autotrophic metabolism over seasonal scales (i.e. Moncoiffé et al., 2000). As a consequence, a surplus of organic matter is available, which can be exported to adjacent systems (Quiñones and Platt, 1991). Given the functional relationship between plankton size structure and the fate of biogenic C, the concurrent analysis of both phytoplankton size structure and net community production provides valuable information on the linkage between the trophic organization of the microbial plankton communities and their potential to recycle organic C within the euphotic layer or to export it to upper trophic levels and adjacent systems.

The Ría de Vigo, the most southerly of the Galician Rías Bajas, is a temperate coastal embayment located in the NW of the Iberian Peninsula. From April to September, this ecosystem is subjected to intense and intermittent upwelling, which increases primary production (Fraga, 1981) and, consequently, the export of biogenic carbon to the sediment and to the adjacent shelf (Prego, 1993; Álvarez-Salgado et al., 2001). During the upwelling favourable period, microphytoplankton (>20 μm) dominate the phytoplankton community, however, nanophytoplankton (<20 μm) have a significant contribution to the total standing stock and primary production (Tilstone et al., 1999). Frequently, a subsurface chlorophyll maximum develops after upwelling, when calm conditions favour water column stratification (Figueiras and Pazos, 1991). From October to March (downwelling favourable season), southerly winds become dominant and enhanced vertical mixing occurs. Previous works have reported that phytoplankton standing stocks and primary production are much lower during this period than during the upwelling favourable season (Fraga, 1976; Nogueira et al., 1997). No previous study has addressed the phytoplankton size structure during winter. In early spring, a transient period between both situations (downwelling–upwelling) gives rise to the onset of spring blooms. On the other hand, the cessation of the upwelling season is characterized by autumn blooms which are typically dominated by dinoflagellates (Figueiras and Ríos, 1993; Tilstone et al., 1994). These overall patterns highlight the hydrographic features of the Ría de Vigo on a seasonal scale. It is well known that this ecosystem also exhibits a large variability on shorter (daily to weekly) time scales (Tilstone et al., 1999). Thus, as a result of the ever changing hydrodynamical conditions, the Ría de Vigo constitutes an ideal scenario to explore the relationship between hydrographic variability, phytoplankton size structure and plankton carbon budgets in microbial pelagic ecosystems.

The seasonal variability of phytoplankton primary production has been scarcely documented in the Galician Rías Bajas. A full annual cycle of primary production in the Ría de Vigo was first covered by Fraga (1976) using the ^{14}C-uptake technique. Subsequently, a seasonal and short-term balance between microbial primary production and respiration has been carried out in this ecosystem by means of the oxygen method (Moncoiffé et al., 2000). This study highlighted the net autotrophic behaviour of this ecosystem throughout the year and its relation to the export potential ability. Further studies of phytoplankton primary production in the Galician Rías Bajas have focused on the analysis of particular oceanographic situations, most commonly during the upwelling season (Hanson et al., 1985; Tilstone et al., 1999).

The relationship between phytoplankton size structure and net community production has been investigated in coastal (e.g. Smith and Kemp, 2001; Teira et al., 2001) and open ocean waters (e.g. Serret et al., 2001; Pérez et al., 2005). To the best of our knowledge no previous study has approached the study of size-fractionated phytoplankton biomass and primary production in conjunction with microbial net community production during an entire annual cycle. From July 2001 to July 2002, the phytoplankton standing stocks and primary production in four size classes, picophytoplankton (0.2–2 μm), small nanophytoplankton (2–5 μm), large nanophytoplankton (5–20 μm) and microphytoplankton (>20 μm) were determined. Simultaneously, the production–respiration balance of the microbial plankton community was also measured in order to build up the plankton carbon budgets during three different oceanographic situations, namely summer stratification, winter mixing and upwelling. Here, we studied how the hydrographic variability on both seasonal and short-time scales affects phytoplankton size structure. Secondly, we investigated, on an empirical basis, the relationship between phytoplankton size structure, food web pathways and the potential fate of biogenic carbon within the microbial plankton community.

2. Material and methods

2.1. Sampling

A total of 25 oceanographic cruises were carried out on board the RV Mytilus to a central station at Ría de Vigo ($42° \, 14.09'$ N, $8° \, 47.18'$ W), where the depth is 45 m in low tide (Fig. 1). Sampling times were scheduled in order to characterize the variability of the system over short (weekly) and seasonal (annual cycle) time scales. Short-time scale studies were distributed in four intensive sampling periods which were composed by 4–6 sampling days, separated by intervals of 2–4 days. During the first intensive sampling period (from 2 to 19 July 2001), a typical summer stratification prevailed. A spring bloom was sampled from 18 to 28 February 2002. Finally, during 11–22 April 2002 and 15–26 July 2002 the oceanographic conditions were characterized by upwelling. In addition to the intensive sampling periods, monthly visits to the Ría were used to obtain a seasonal cycle that extended from July 2001 to July 2002.

2.2. Hydrography and irradiance

On each visit, vertical profiles (0–40 m) of temperature and conductivity were recorded with a SeaBird Electronics 25 CTD probe. Prior to the sampling, the vertical distribution of photosynthetically active irradiance (PAR, 400–700 nm) was measured with a spherical quantum sensor connected to a LiCor datalogger. Seawater samples for chemical and biological measurements were collected using a 5-L Niskin bottle. Samples for the analysis of dissolved inorganic nutrients (nitrate, nitrite, ammonia, phosphate and silicate) were obtained from surface, 5, 10, 15, 20 and 30 m. These samples were immediately frozen and stored at $-20 °C$ until they were analysed in the laboratory by segmented flow analysis with Alpkem autoanalysers following Hansen and Grasshoff (1983) with some improvements (Mouriño and Fraga, 1985).

Ekman transport ($-Q_x$), an estimate of the water flow ($m^3 \, s^{-1}$) upwelled per kilometre of coast, was calculated according to Wooster et al. (1976):

$$-Q_x = \frac{\rho_a C |V|}{f \rho_w} V_H$$

where ρ_a is the density of air at 15 °C (1.22 kg m^{-3}); C is an empirical drag coefficient (dimensionless), 1.3×10^{-3}; f is the Coriolis parameter at 43° latitude (9.9×10^{-5} s^{-1}); ρ_w is the density of seawater (~ 1025 kg m^{-3}); V is wind speed and V_H is the component of wind speed parallel to the coast, as the coastline is rotated $\sim 15°$ regarding the N–S axis. Geostrophic winds were calculated from surface pressure charts at 43°N, 11°W. Positive values of $-Q_x$ indicate upwelling favourable offshore Ekman transport, and negative values of $-Q_x$ indicate downwelling favourable onshore Ekman transport.

2.3. Size-fractionated chlorophyll a

Samples for the determination of biological variables were collected at surface, 5, 10, 15 and 20 m depth. Samples were stored in acid-washed, black polypropylene carboys and transported to the laboratory within 2 h of sampling. Special care was taken to avoid any light shock to the plankton populations. Size-fractionated chlorophyll *a* (Chl *a*) concentration was determined on replicate 250 ml samples, which were filtered sequentially through 20, 5, 2 and 0.2 μm pore size polycarbonate filters. Cells retained by the 20 μm filters belong to the microphytoplankton whereas those retained by the 2 and 0.2 μm pore size constitute, respectively, nanophytoplankton and picophytoplankton. Small (2–5 μm) and large nanophytoplankton
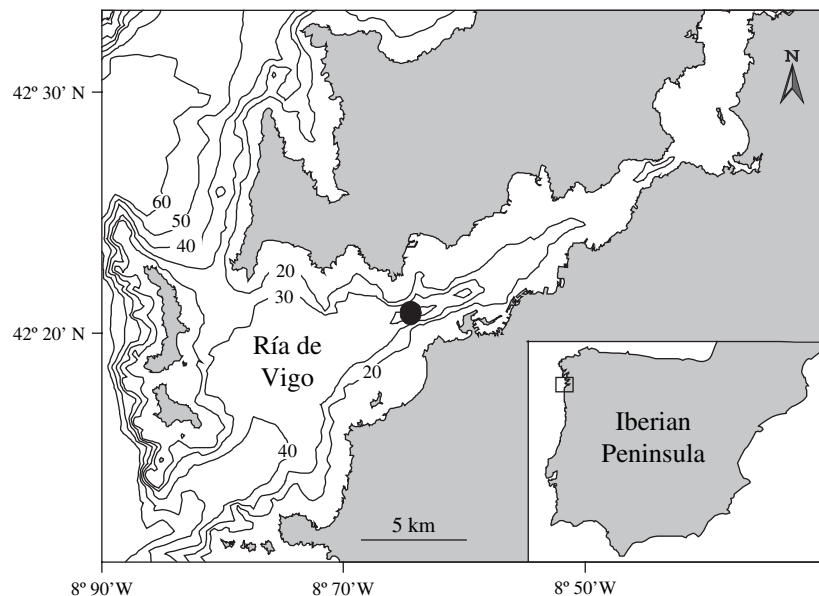

Fig. 1. Map of the study area and sampling station.

(5−20 μm) size fractions were also differentiated. After filtration, pigments were extracted in 90% acetone for 24 h in the dark and at 4 °C. Chl *a* concentration was determined fluorometrically without acidification with a Turner Designs Fluorometer (TD-700) which had been calibrated with pure Chl *a* (Sigma).

2.4. Size-fractionated particulate organic carbon production (POC-pr)

Size-fractionated particulate organic carbon production rates (POC-pr) were determined by running simulated 'in situ' incubations with the radioisotope ^{14}C. Four 75 ml acid-washed polystyrene bottles (three light and 1 dark bottle) were filled with seawater from surface, 5,10, 15 and 20 m depth. Each bottle was inoculated with ∼370 kBq (10 μCi) of $NaH^{14}CO_3$ and then incubated for 2 h starting at noon. An incubator equipped with a set of blue and neutral density plastic filters was used. This incubator reproduced the irradiance conditions at the original depths where the samples had been collected. A system of re-circulating water passing through two refrigerators was used to maintain incubation temperature within 1.5 °C of the original temperature at each sampling depth.

At the end of the incubations, samples for the determination of POC-pr were sequentially filtered through 20, 5, 2 and 0.2 μm polycarbonate filters under low-vacuum pressure (<100 mm Hg). Inorganic carbon on the filters was removed by exposing them to concentrated HCl fumes overnight. After removal of inorganic ^{14}C, filters were placed into scintillation vials to which 4 ml of scintillation cocktail were added. The radioactivity on each sample was determined on a 1409-012 Wallac scintillation counter which used an internal standard for quenching correction. Dark bottle disintegrations per minute (DPMs) were subtracted from the light bottle DPMs in order to calculate POC-pr.

2.5. Dissolved organic carbon production (DOC-pr)

Simultaneously to the measurement of POC-pr, the production rate of dissolved organic carbon (DOC-pr) was determined. This methodology has previously been described in detail by Marañón et al. (2004). For each sampling depth (0, 10 and 20 m), three light and two dark acid-washed, Pyrex glass bottles (36 ml in volume) were filled with the sample and spiked with 15 μCi (555 kBq) of $NaH^{14}CO_3$. Sample incubation was identical to that previously described for the determination of POC-pr.

At the end of the incubation, two 5-ml samples from each bottle were filtered through 0.2 μm polycarbonate filters under low-vacuum pressure (<50 mm Hg). After being acidified to pH ∼2 with 100 μl of 18.5% HCl, filtrates were kept for 12 h in open scintillation vials (20 ml in volume) placed on an orbital shaker. After ^{14}C decontamination, 15 ml of a high sample capacity scintillation cocktail were added to each filtrate. The inorganic ^{14}C present in the filters was removed by exposing them to concentrated HCl fumes for

12 h. Sample processing and production calculations were done as previously described for POC-pr samples.

2.6. Community photosynthesis and respiration

Gross primary production (GPP), net community production (NCP) and dark community respiration (DCR) were determined at three depths (0, 10 and 20 m) from in vitro changes in dissolved oxygen after light and dark bottle incubations. Additional samples were taken at 30 m depth for DCR determination. Twelve 120 ml, gravimetrically calibrated, acid-washed borosilicate glass bottles were carefully filled from each carboy by means of a silicone tube, overflowing by >250 ml and taking precautions to minimise sample exposure to light or temperature changes. From each depth, four replicate bottles were fixed immediately for initial oxygen concentrations, four bottles were kept in darkness and four bottles incubated under the same conditions than those used for the ^{14}C incubations. After the 24 h incubation period, dissolved oxygen concentration was determined according to the method of Grasshoff (1976). Measurements of dissolved oxygen were made with an automated Winkler titration system Metrohm 721 Net Titrino, using a potentiometric end point. Aliquots of fixed samples were delivered with a 50-ml overflow pipette. Production and respiration rates were calculated as follows: NCP = ΔO_2 in light bottles (mean [O_2] in 24 h light − mean initial [O_2]); DCR = ΔO_2 in dark bottles (mean initial [O_2] − mean [O_2] in 24 h dark); GPP = NCP + DCR.

3. Results

3.1. Hydrographic conditions

The seasonal variability of the Ekman transport during the study period is shown in Fig. 2a. In general, positive values were observed during the upwelling favourable season (July 2001−September 2001 and April 2002−July 2002) and negative values during the downwelling favourable season (October 2001−March 2002). According to these general patterns, vertical profiles of temperature (Fig. 2b) and salinity (Fig. 2c) illustrate the two contrasting hydrographic situations. Water column stratification prevailed during the upwelling favourable season with surface temperatures that varied between 15 and 18 °C, decreasing to 13.5 °C below the thermocline located at 5−10 m depth. During pronounced upwelling pulses (e.g. 5 September 2001), the 14 °C isotherm reached the surface giving rise to a strong vertical mixing. Winter and autumn conditions were characterized by thermal homogeneity of the water column due to continuous vertical mixing. During this period temperature values were in the range 13−15 °C and salinity was typically lower at surface, due to continental runoff. During the November cruise, temperatures around 17 °C were measured in the entire water column, which was associated with the intrusion of subtropical water masses from the adjacent shelf. Thermal inversions maintained by saline stratification in the uppermost layer were observed on 5 November 2001, 31 January 2002 and 18−28
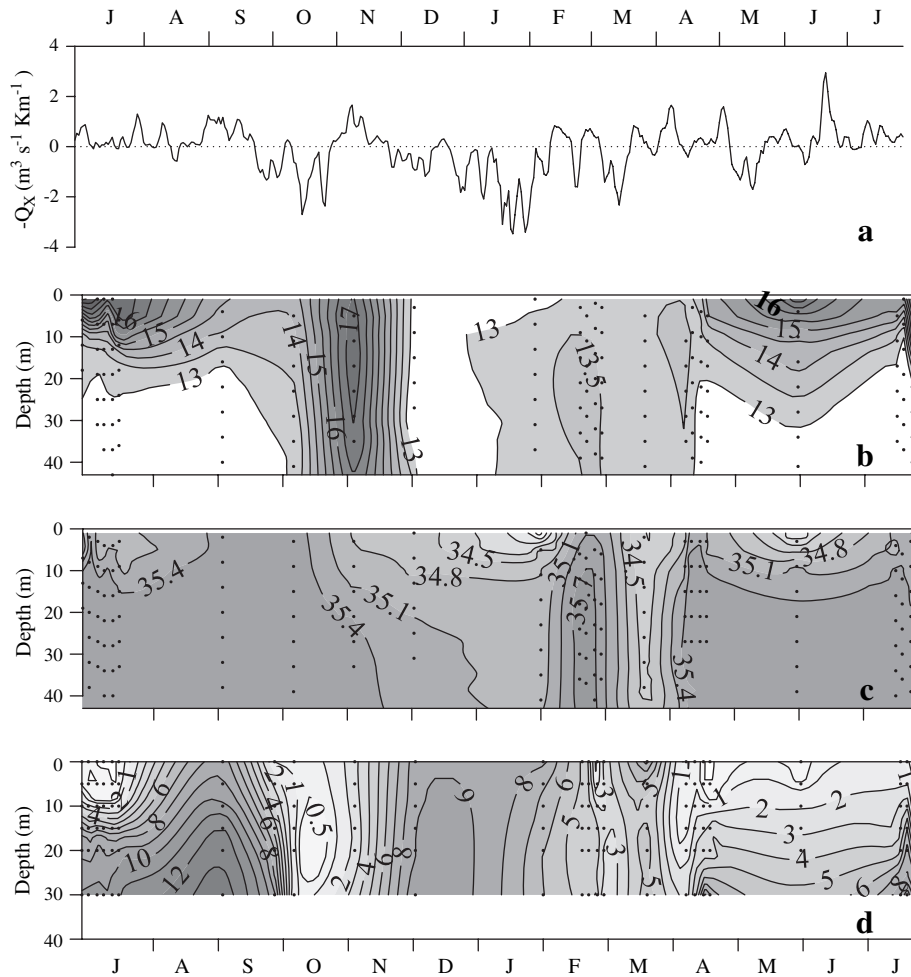
Fig. 2. (a) Time course of the west−east component of the Ekman transport ($-Q_x$, in $m^3\,s^{-1}\,km^{-1}$) averaged from three previous days and vertical distribution of (b) temperature (°C), (c) salinity and (d) nitrate concentrations ($\mu mol\,l^{-1}$) from July 2001 to July 2002.

February 2002. Thermal inversion is a common feature of this system during late autumn, winter and spring, when the supply of cold and fresh waters by continental runoff increases. In early spring, a subsurface saline stratification followed by the upwelling of nutrient-rich deep waters triggered the onset of the spring phytoplankton bloom on 25 February.

Surface nutrient concentrations were low in summer and high in winter (Fig. 2d). In summer, upwelling pulses increased nutrient levels in the euphotic layer (from surface to 20 m, ~1% optical depth) but subsequent consumption by phytoplankton occurred during extended relaxation and stratification periods. Thus, after an upwelling pulse, nutrient levels in surface waters were exhausted, but remained high at the base of the euphotic layer where a marked nutricline developed. In general, during pronounced upwelling pulses, nitrate concentrations were as high as 10 $\mu mol\,L^{-1}$ at 20 m depth and >8 $\mu mol\,L^{-1}$ at the surface. In winter, nutrients were high and homogenously distributed throughout the water column. During this period, nitrate, silicate and phosphate concentrations were in the range 5−8, 5−7 and 0.4−0.65 $\mu mol\,L^{-1}$, respectively.

3.2. Seasonal patterns of total and size-fractionated chlorophyll a

Chl *a* concentration was higher in summer than in winter (Fig. 3). In general, the vertical distribution of Chl *a* was characterized by a surface maximum and a progressive decrease with depth. Contrarily to this overall pattern, during summer stratification a typical subsurface Chl *a* maximum developed at about 10 m. Likewise, during post-bloom stages (i.e. 28 February 2001), high Chl *a* concentrations were measured at the bottom of the euphotic layer. Typically, the four size fractions showed maximum values of Chl *a* at the surface. However, in relative terms, small-sized phytoplankton increased their contribution to total Chl *a* with depth (Fig. 3).

Total euphotic layer integrated Chl *a* varied from 10.5 to 27.2 mg Chl *a* m^{-2} during the downwelling favourable season (spring bloom excluded), and from 35.7 to 128.9 mg Chl *a* m^{-2} during the upwelling season (Fig. 4a). During upwelling, microphytoplankton were the dominant size class, accounting for more than 80% of total Chl *a* (Fig. 4a). The highest Chl *a* concentrations in the >20 μm size fraction were
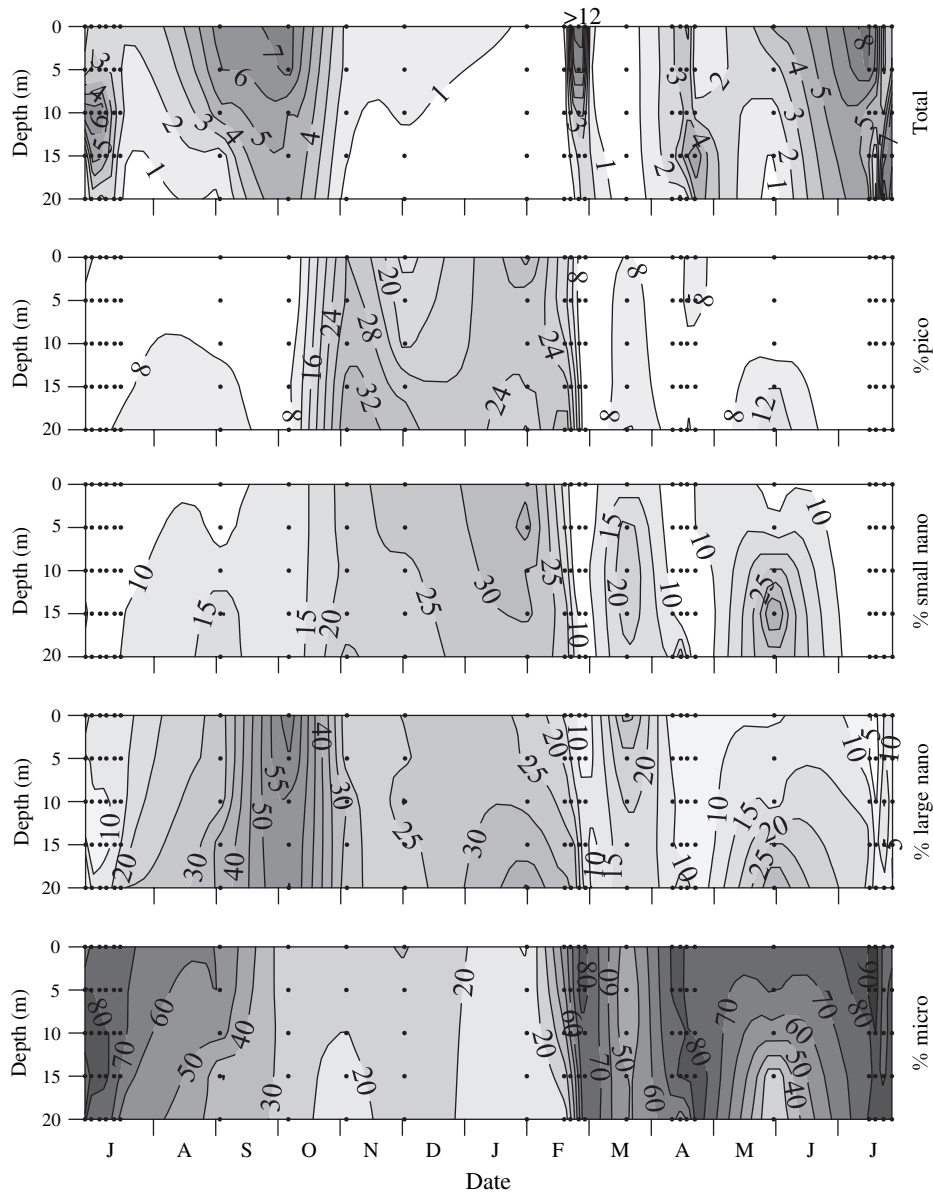
Fig. 3. Vertical distribution of total Chl *a* concentration (mg Chl *a* m^{-3}) and the contribution (%) of each size fraction to the total Chl *a* from July 2001 to July 2002.

measured at the surface in early spring and summer, associated with the spring bloom and summer upwelling (12 and 7.6 mg Chl *a* m^{-3}, respectively). The contribution of <20 μm phytoplankton to total Chl *a* increased during the downwelling favourable season, when it represented more than 70% of total Chl *a* (Fig. 4a). Picophytoplankton Chl *a* showed relatively constant values all year round. However, their relative contribution to total Chl *a* was highly variable, accounting for less than 10% during the upwelling favourable season but as much as 30% during the intrusion of subtropical waters in the November cruise (Fig. 4a). Similarly, large and small nanophytoplankton showed low, relatively constant concentrations throughout the year, with enhanced relative contributions to total Chl *a* during autumn and winter (Fig. 3).

3.3. Seasonal patterns of total and size-fractionated POC-pr

POC-pr showed a seasonal pattern close to that of Chl *a* (Fig. 5). Chl *a* concentration and POC-pr in the uppermost euphotic layer varied seasonally by one and two orders of magnitude, respectively. However, the photosynthesis to Chl *a* ratio exhibited a relatively low variability throughout the study (from 1.5 to 10.8 mg C mg Chl *a*$^{-1}$ h^{-1} in surface), which indicates that both variables were coupled tightly. Higher POC-pr rates were measured at the surface during the summer upwelling and the spring bloom (82 and 110 mg C m^{-3} h^{-1}, respectively) whereas lower rates were observed in winter (1.65 mg C m^{-3} h^{-1} in March). Total euphotic layer integrated POC-pr varied from 22.4 to 97.5 mg C m^{-2} h^{-1} during the
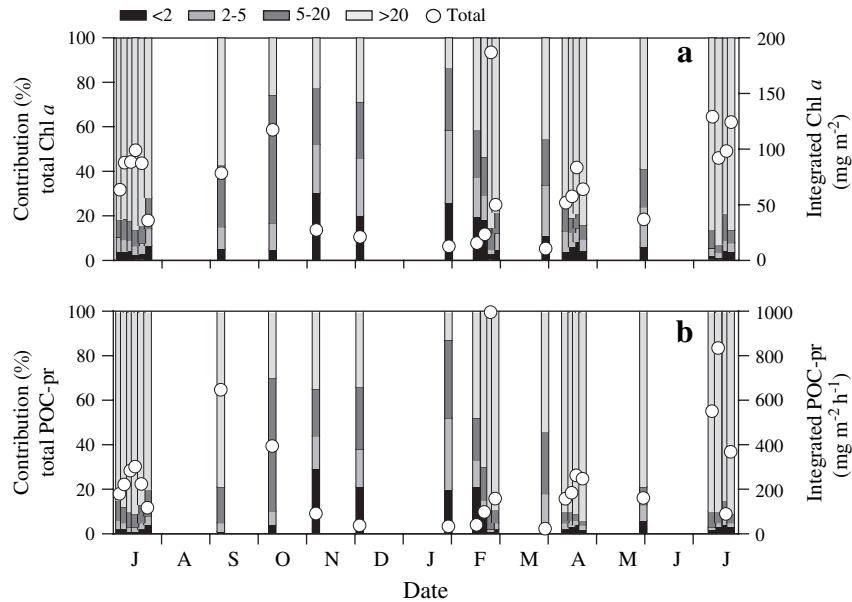
Fig. 4. Seasonal variability (July 2001–July 2002) of (a) total euphotic layer integrated Chl a concentration (mg Chl a m^{-2}, circles) and the contribution (%) of each size fraction to total Chl a (bars) and (b) total euphotic layer integrated POC-pr (mg C m^{-2} h^{-1}, circles) and the contribution (%) of each size fraction to total POC-pr (bars).

downwelling favourable season (spring bloom excluded), and from 88.6 to 834 mg C m^{-2} h^{-1} during the upwelling season (Fig. 4b). During the spring bloom, we measured a total POC-pr as high as 995 mg C m^{-2} h^{-1}. However, in terms of daily rates, pronounced upwelling events were more productive due to the longer photoperiod. The microphytoplankton size fraction dominated during the upwelling favourable season and the spring bloom, accounting for more than 80% of total POC-pr (Fig. 4b). The remaining 20% was accounted mainly for the large nanophytoplankton with a minor contribution of the small nano- and picophytoplankton size fractions. From October 2001 to March 2002, the microphytoplankton contributed less than 40% to total POC-pr rates except during the early spring bloom. On average, POC-pr rates by picophytoplankton were low throughout the study period but showed some degree of variability within this background level. For example, during November and the pronounced upwelling in July 2002, POC-pr rates by picophytoplankton were as high as 19 and 22.5 mg C m^{-2} h^{-1}, respectively (Fig. 4b). In contrast during March 2002, POC-pr by picophytoplankton did not exceed 1 mg C m^{-2} h^{-1}. In relative terms, the contribution of picophytoplankton to total POC-pr was around 5 and 30% during summer upwelling and winter mixing, respectively.

The vertical variability of POC-pr reflected the vertical distribution of Chl a. More than 60% of the total euphotic layer integrated POC-pr rates (from surface to 20 m, ~1% optical depth) were measured in the upper 10 m of the water column throughout the study period (Fig. 5). During pronounced upwelling pulses in September 2001 and July 2002 and during the spring bloom, more than 80% of the total euphotic layer integrated POC-pr occurred in the upper 10 m of the water column. Similar to the pattern observed for Chl a, the

contribution of small-sized cells (<20 μm) to total POC-pr increased with depth (Fig. 5). This vertical pattern was associated with a decrease in biomass and POC-pr of large-sized phytoplankton rather than by an increase in biomass and POC-pr of the smaller fractions.

3.4. Short-scale variability of size-fractionated Chl a and POC-pr

3.4.1. Stratification

A persistent stratification took place during the intensive sampling period carried out from 2 to 19 July 2001. A marked thermocline was located at roughly 5 m throughout this period (Fig. 6a). Nutrient concentrations were low above the thermocline whereas higher concentrations were measured in deeper waters (Fig. 6b). This situation was characterized by the presence of a subsurface chlorophyll maximum (SCM), dominated by microphytoplankton, at 10 m. From 2 to 9 July northerly winds enhanced positive estuarine circulation (see Fig. 2a). This brought nutrients up to the base of the thermocline, thus enhancing POC-pr at the SCM. As a result, on 12th July Chl a concentration reached 9.9 mg m^{-3} at 10 m depth and POC-pr was as high as 24 mg C m^{-3} h^{-1} (Fig. 6c, d). Strong stratification prevented the fertilisation of the uppermost layer and low Chl a concentrations (1.5–3 mg Chl a m^{-3}) and POC-pr (5.5–23.5 mg C m^{-3} h^{-1}) were measured at the surface. During the whole sampling period, the phytoplankton community was dominated by the >20 μm size fraction, which accounted for up to 86 and 91% of total Chl a and POC-pr, respectively (Fig. 6e, f). After 12th July the cessation of northerly winds gave rise to the passive sedimentation of the SCM. Chl a concentrations and POC-pr in the >20 μm

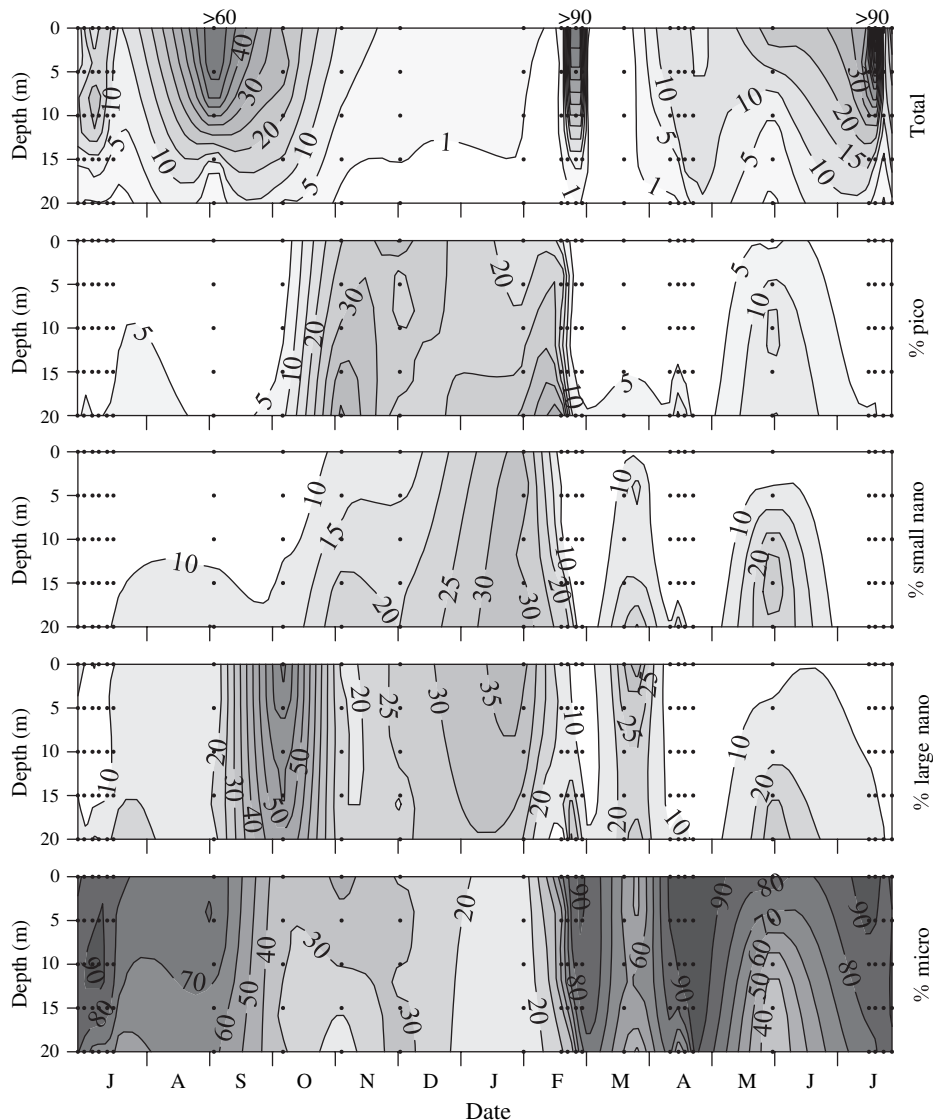Fig. 5. Vertical distribution of total POC-pr (mg C m^{-3} h^{-1}) and the contribution (%) of each size fraction to total POC-pr from July 2001 to July 2002.

size fraction diminished progressively whereas scarce changes were observed in the smaller size fractions.

3.4.2. Spring bloom

From 18 to 21 February 2002 thermal inversions, maintained by saline stratification, characterized the hydrography of the water column (Fig. 7a). Temperature in surface waters increased from 13 to 13.5 °C throughout this intensive sampling period. Nutrients were distributed homogeneously in the entire water column with nitrate concentrations in the range of 4.5–5 μmol L^{-1} (Fig. 7b). Total euphotic layer integrated Chl a concentrations and POC-pr rates never exceeded 1 mg m^{-2} and 0.1 g C m^{-2} h^{-1}, respectively. At the beginning of this sampling period, the phytoplankton size structure was characterized by a substantial contribution (>50%) by pico- and nanophytoplankton to total Chl a and POC-pr rate. On February 21st, >20 μm cells increased conspicuously their contribution to total Chl a and POC-pr. On 25 February, an

intense saline stratification in the uppermost water column induced the onset of the spring phytoplankton bloom, which was dominated by the small, chain-forming diatom *Skeletonema costatum* (F. G. Figueiras, personal communication). Chl a concentration and POC-pr rates at surface reached 16 mg m^{-3} and 0.99 g C m^3 h^{-1}, respectively, during the development of the bloom (Fig. 7c, d). The phytoplankton size structure shifted drastically to be dominated by >20 μm cells, which accounted for more than 90% of total Chl a and POC-pr (Fig. 7e, f). Picophytoplankton and nanophytoplankton size fractions also showed a slight increase in their respective Chl a concentrations and POC-pr rates, but their relative contribution to total biomass and production decreased.

3.4.3. Upwelling episodes

The intensive sampling periods from 11 to 22 April 2002 and from 15 to 26 July 2002 represented two upwelling relaxation sequences. By 11 April a slight thermal inversion
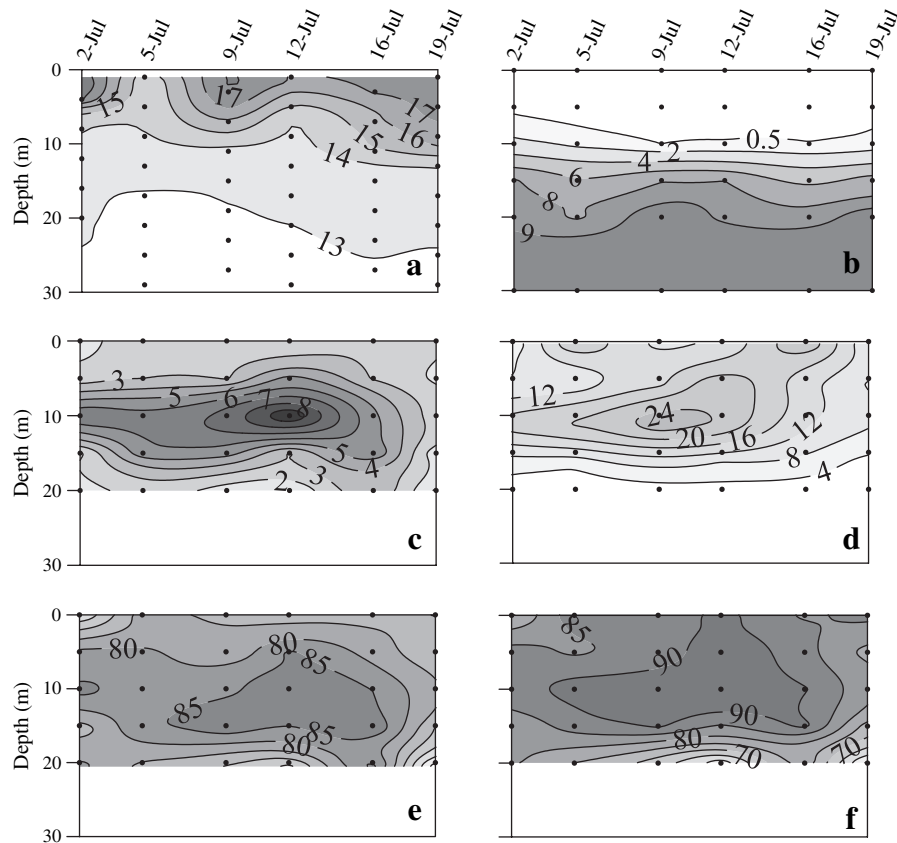
Fig. 6. Vertical distribution of (a) temperature (°C), (b) nitrate concentration (μmol l^{-1}), (c) total Chl a concentration (mg Chl a m^{-3}), (d) total POC-pr (mg C m^{-3} h^{-1}) and the contribution (%) of microphytoplankton to total (e) Chl a and (f) POC-pr during the intensive sampling carried out from 2 to 19 July 2001.

(Fig. 8a) was maintained by saline stratification. This situation was characterized by low nitrate concentrations in the uppermost euphotic layer (Fig. 8b) and low Chl a and POC-pr throughout the water column (Fig. 8c, d). Subsequently, northerly winds resulted in upwelling of cold, nutrient-rich deep waters. This phenomenon gave rise to the increase of phytoplankton biomass and POC-pr during the next days. At the surface, maximum Chl a concentrations and POC-pr exceeded 4 mg Chl a m^{-3} and 15 mg C m^{-3} h^{-1}, respectively. By 22 April, upwelling ceased, surface temperature increased and water column stratification developed, favouring the sedimentation of phytoplankton biomass under calm wind conditions. As a result, high Chl a concentration (6 mg Chl a m^{-3}) and POC-pr (18 mg C m^{-3} h^{-1}) were measured at 15 m depth (Fig. 8c, d) on 22nd April. During the July cruise, the sequence was similar but after the upwelling relaxation a new upwelling of cold and nitrate-rich waters (Fig. 9a, b) caused an increase of phytoplankton biomass and POC-pr (Fig. 9c, d). In this case, nitrate was exhausted completely in surface waters, which coincided with an increase of Chl a and POC-pr rates that exceeded 8 mg Chl a m^{-3} and 70 mg C m^{-3} h^{-1}, respectively. In both cases, the size structure of the phytoplankton community was dominated by >20 μm phytoplankton cells, which accounted persistently for more than 70 and 80% of the total Chl a and POC-pr, respectively (Figs. 8e, f and 9e, f).

3.5. Chl a biomass and production of small and large phytoplankton

All 25 determinations of the relative contribution of small and large phytoplankton to total euphotic layer integrated Chl a concentration and POC-pr rate, have been plotted on Fig. 10 following the approach proposed by Tremblay and Legendre (1994). In essence, when data points are above the main diagonal, the relative contribution of large phytoplankton to total production is higher than their share of Chl a biomass. In this work, a mean cell size of 5 μm diameter was used to separate small and large phytoplankton. This limit has been suggested by different authors as the lower smallest cell size on which mesozooplankton predate efficiently, and therefore bears considerable ecological implications (Legendre and Rassoulzadegan, 1996). All data points corresponding to the upwelling favourable conditions were closely grouped in the upper right corner of the production–biomass plot, indicating the dominance of large cells in terms of both biomass and POC-pr rates. Points corresponding to the winter mixing were displaced towards the middle of the plot, indicating that during this period the relative contribution of larger cells to both total biomass and POC-pr decreased. Despite the wide changes in the absolute values of size-fractionated Chl a concentration and POC-pr, all data points fell consistently above the main diagonal, indicating that the relative contribution of
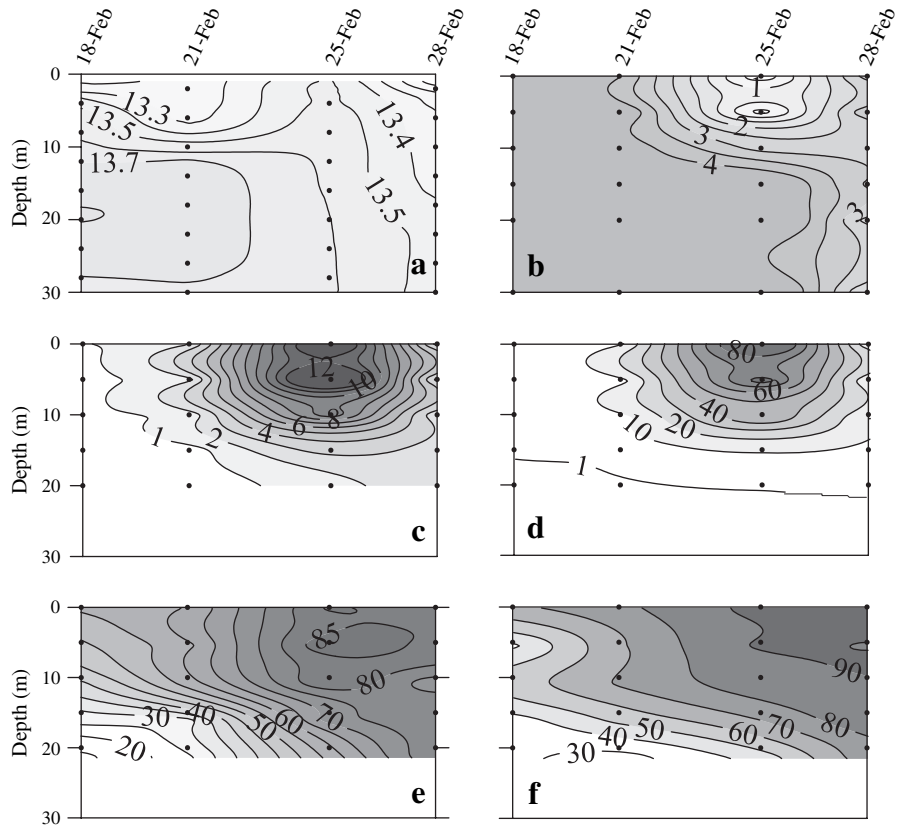
Fig. 7. As Fig. 6 but for the intensive sampling carried out from 18 to 28 February 2002.
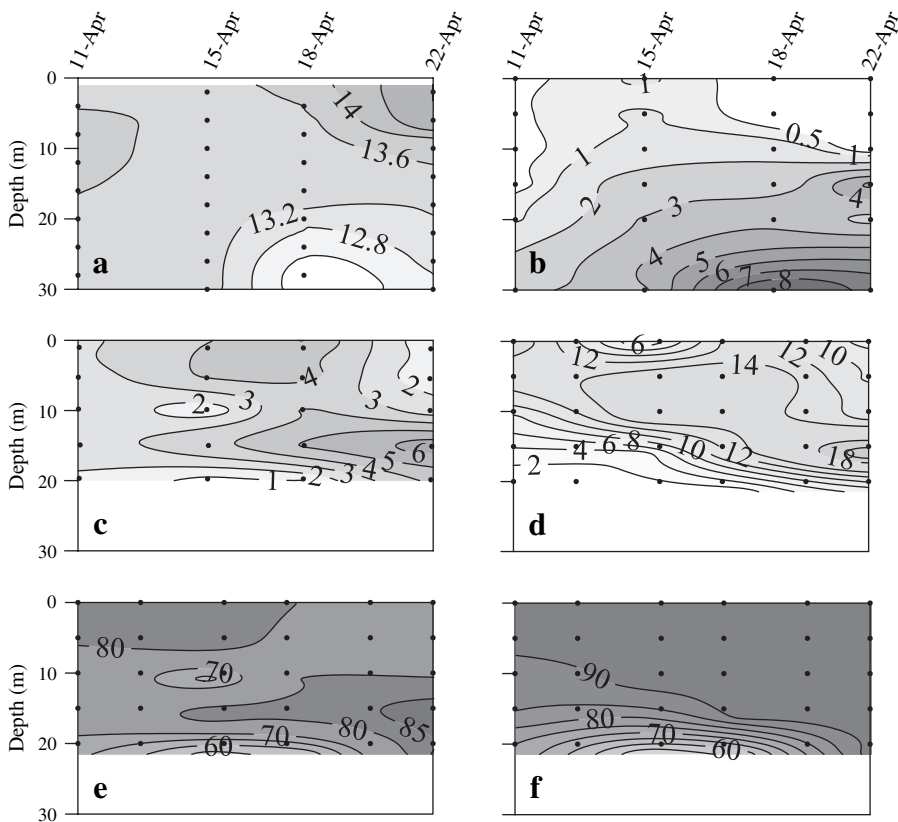

Fig. 8. As Fig. 6 but for the intensive sampling carried out from 11 to 22 April 2002.
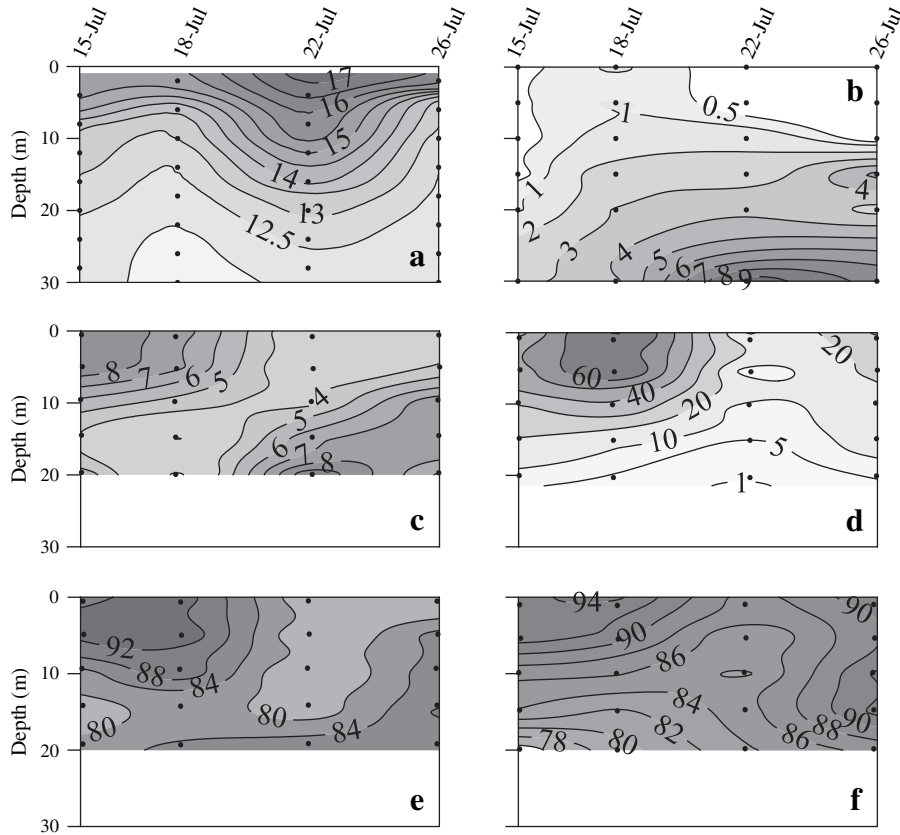
Fig. 9. As Fig. 6 but for the intensive sampling carried out from 15–26 July 2002.

>5 μm phytoplankton to total production was higher than their share of Chl *a* biomass.

3.6. Planktonic carbon budgets

Using the measurements presented so far as well as data on dissolved organic carbon production (DOC-pr) and oxygen
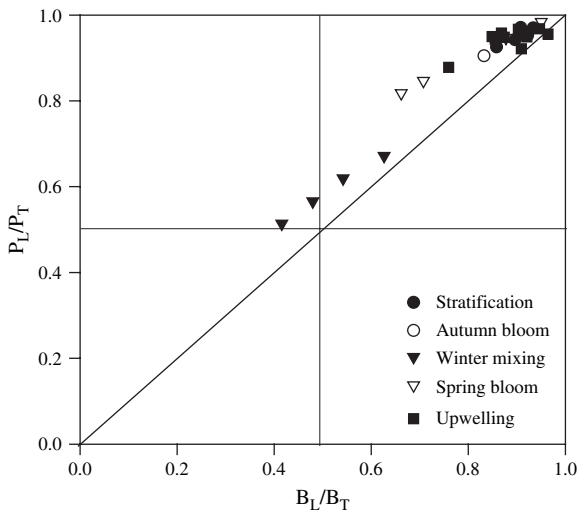

Fig. 10. Relationship between the contribution of large (>5 μm) phytoplankton to total community phytoplankton biomass (B_L/B_T) and primary production (P_L/P_T).

production and consumption, all simultaneously measured during this annual cycle, the carbon budget in the microbial plankton community has been built during three contrasting oceanographic situations: summer stratification, winter mixing and upwelling. Phytoplankton standing stocks are represented as carbon biomass obtained from Chl *a* data and size-fractionated C to Chl *a* estimates (Cermeño et al., 2005a). These C to Chl *a* ratios were obtained using estimates of phytoplankton abundance and cell volume from flow cytometry and microscopy analysis. Cell volume was converted to carbon biomass using volume to carbon conversion factors taken from the literature. Finally, size-fractionated C biomass was divided by Chl *a* concentrations. Gross primary production and respiration rates estimated by the oxygen method were converted to carbon units by using photosynthetic and respiratory quotients of 1.4 and 1, respectively (Fraga, 1976; Packard, 1979). The size-fractionated gross photosynthesis rates were obtained by applying the contribution percentages of ^{14}C-uptake estimates to the gross primary production rates estimated from the oxygen method. Although photosynthetic and respiratory quotients may vary with a number of factors such as the physiological status of phytoplankton cells, our purpose was to provide an overall insight into the main pathways of carbon transfer within the microbial pelagic community rather than an exhaustive quantitative analysis of plankton carbon budgets. The seasonal and short-scale variability of the oxygen fluxes will be described in detail in a separate report.

Carbon stocks and flows within the microbial plankton community during summer stratification, winter mixing and upwelling are shown in Fig. 11. During summer stratification and upwelling, high rates of total POC-pr were associated with high standing stocks, contributed mainly by the microphytoplankton size class. During winter mixing, low biomass and POC-pr were associated with the co-dominance of small- and large-sized cells. The seasonal and short-scale variability of the dissolved organic carbon production (DOC-pr) by phytoplankton assemblages in the Ría de Vigo has been described in Marañón et al. (2004). DOC-pr accounted for a significant fraction of the total organic carbon production
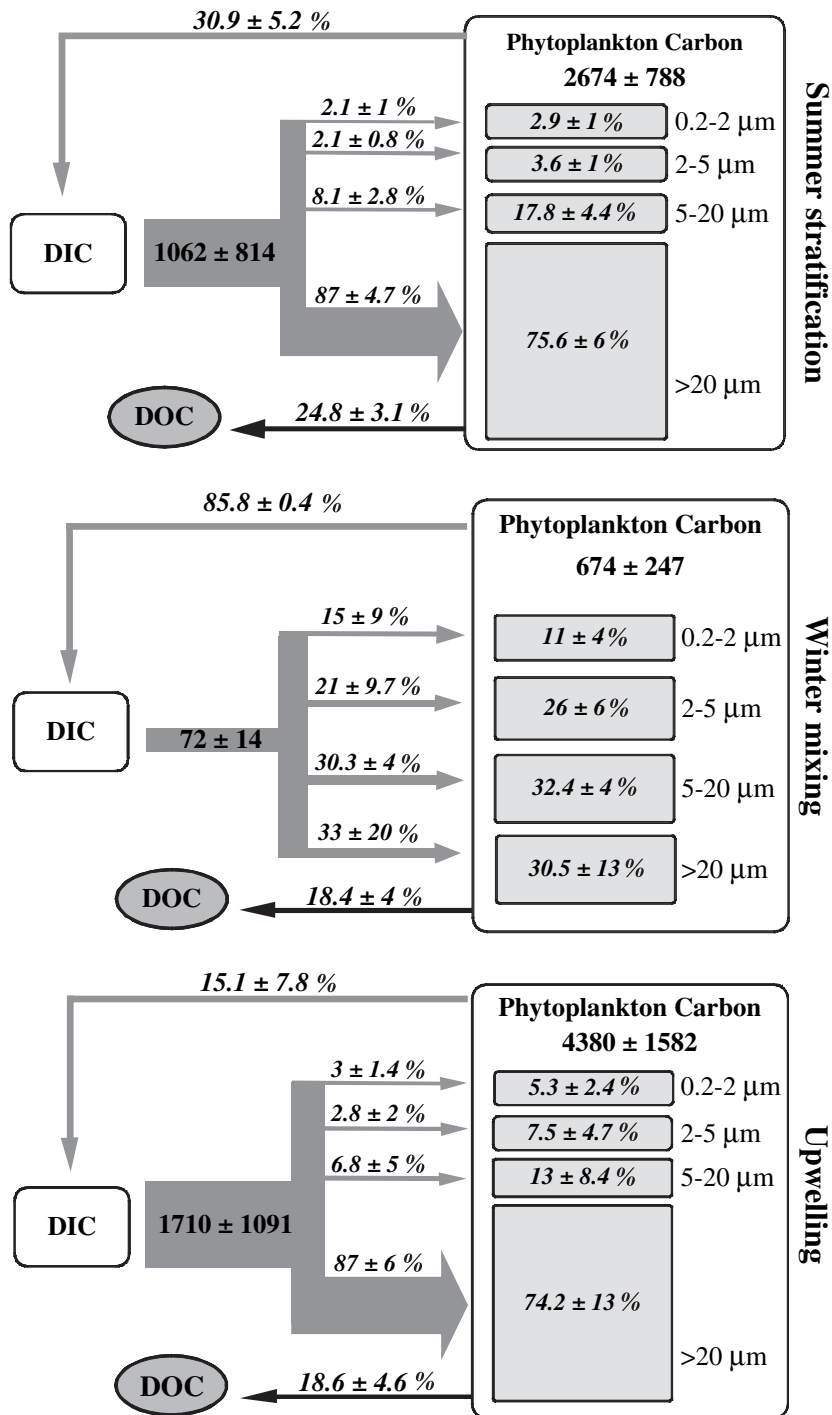

Fig. 11. Microbial plankton carbon budgets during three contrasting oceanographic situations: summer stratification, winter mixing, and upwelling. Phytoplankton biomass is expressed in mg C m^{-2} (±standard deviation). C flows are expressed in mg C m^{-2} d^{-1} (±sd). Boldfaced numbers represent absolute values of euphotic layer integrated gross photosynthesis and phytoplankton carbon biomass. Figures in italics represent the relative contribution of any given flow or phytoplankton size fraction to total gross primary production or total phytoplankton carbon. Note that the C return flow to dissolved inorganic carbon (DIC) represents respiration by the whole microbial plankton community. See Section 3.6 for details on calculations and conversion factors.

(TOC-pr = POC-pr + DOC-pr). The contribution of DOC-pr to euphotic layer integrated TOC-pr ranged between ∼25% during summer stratification and ∼18% during winter and upwelling conditions. Community respiration varied conspicuously in the three contrasting oceanographic situations. In absolute values, the highest microbial respiration rates (mean standard deviation) were measured during summer stratification (324 ± 264 mg C m^{-2} d^{-1}) whereas community respiration was as low as 62 ± 15 mg C m^{-2} d^{-1} during winter mixing. In relative terms, however, microbial community respiration consumed 86% of the total primary production during winter. During summer stratification and upwelling, respiration represented only 31 and 15%, respectively, of total primary production.

4. Discussion

4.1. Seasonal variability of Chl a concentration and POC-pr

The seasonal evolution of the hydrographic variables and phytoplankton biomass observed in this study followed a similar pattern to those previously described in the Galician Rías Bajas (Álvarez-Salgado et al., 1996; Nogueira et al., 1997; Moncoiffé et al., 2000). Total euphotic layer integrated Chl *a* concentrations were in the range of those reported previously in the Ría de Vigo (Nogueira et al., 1997; Álvarez et al., 1999). Our estimates of POC-pr, however, differed significantly from previous data reported for the Galician Rías Bajas. Assuming a constant photoperiod of 10 h, our study yielded an average value of total euphotic layer integrated POC-pr of 1.4 ± 1.2 g C m^{-2} d^{-1}, and thus a year-integrated value of 520 g C m^{-2} y^{-1}. This value is close to 560 g C m^{-2} y^{-1}, calculated by means of trapezoidal integration of POC-pr values obtained from July 2001 to July 2002. In both cases, our annual estimates are higher than 260 g C m^{-2} y^{-1}, reported by Fraga (1976) for an inner station of the Ría de Vigo. Fraga (1976) used a photoperiod of 12 h but taking into account that carbon fixation rate is not constant throughout the day. Thus, the discrepancy may be due to methodological differences between both studies, but can also reflect interannual variability in primary production.

The seasonal patterns of size-fractionated Chl *a* and POC-pr observed in our study showed two contrasting situations, associated with different hydrographic regimes. The upwelling season was characterized by high levels of Chl *a* concentrations and primary production and a strong dominance of large-sized phytoplankton. By contrast, the downwelling season was characterized by low Chl *a* concentrations and production rates and a relatively balanced contribution of small and large phytoplankton to total standing stocks and primary production. The cessation and the beginning of the upwelling season were characterized by phytoplankton blooms which gave rise to marked changes in phytoplankton size structure. In the following sections we discuss the relationship between the hydrographic conditions and the variability in the size structure of phytoplankton.

4.2. Dominance of large-sized phytoplankton during the upwelling season

Phytoplankton size structure during the upwelling favourable season differed from that observed during winter in terms of total biomass, POC-pr as well as in the relative contribution of each size fraction. Numerous studies in coastal regions have reported that phytoplankton size structure is characterized by the persistence of <5 μm phytoplankton cells, upon which blooms of larger cells are superimposed when significant inputs of nutrients take place (Riegman et al., 1993; Tremblay et al., 1997; Tamigneaux et al., 1999). Under favourable conditions, large-sized phytoplankton respond with enhanced growth rates and often give rise to important biomass accumulations. By contrast, the biomass and production of small phytoplankton are controlled more strictly by microzooplankton grazing, thus making large blooms of smaller cells less frequent (Kiørboe, 1993). Typically, these transient situations give rise newly to shifts in the phytoplankton size structure which returns to be dominated by small-sized cells whenever nutrients are exhausted and large cells decline. In our study, the short-scale variability (days to weeks) of the hydrographic conditions provides a feasible explanation for the continuous dominance of larger phytoplankton during the upwelling season. Upwelling intermittency is an important feature of the Galician Rías Baixas, which has been shown to affect phytoplankton species succession (Figueiras and Niell, 1987; Figueiras and Ríos, 1993). In these systems, the hydrographic regime between two consecutive upwelling events is characterized by relaxation and stratification under low-wind forced conditions. This sequence (upwelling–relaxation–stratification), which lasts usually for 2–3 weeks, prevails throughout the upwelling season (Blanton et al., 1987; Álvarez-Salgado et al., 1993) and was investigated during the intensive sampling periods carried out in July 2001, April 2002 and July 2002. Consistently, throughout these sampling periods, the phytoplankton community was characterized by high standing stocks and POC-pr, and a marked dominance by >20 μm phytoplankton cells (>55 and >75% of total Chl *a* and POC-pr, respectively).

The species succession characteristic of the upwelling relaxation–stratification has been described before for these waters (Figueiras and Niell, 1987; Figueiras and Ríos, 1993; Tilstone et al., 2000). Typically, small, chain-forming diatoms dominate the upwelled waters. Subsequent transient periods are dominated by flagellates and larger diatoms during relaxation and stratification. Persistent stratification gives rise to the development of a subsurface chlorophyll maximum below the thermocline. This situation may be maintained by a continuous input of nutrients through vertical diffusion from below the sharp nutricline at the base of the euphotic layer as well as by a weak positive estuarine circulation (Figueiras and Pazos, 1991).

In summary, the intermittency of the upwelling, the higher photosynthetic efficiency of large-sized phytoplankton under high nutrient and irradiance conditions (see below), and, presumably, the trophic mismatch between larger phytoplankton

and mesozooplankton are likely to account for the continuous dominance of large-sized phytoplankton during the upwelling favourable season.

4.3. Phytoplankton size structure during the downwelling season

During winter mixing, picophytoplankton contribution to total Chl *a* and POC-pr reached values as high as 30 and 28%, respectively. These values were significantly higher than those obtained during the upwelling favourable season (<5% to total Chl *a* and POC-pr). In November, typical winter conditions, with a well-mixed water column were encountered. However, relatively high temperatures and low nutrient concentrations suggested the onshore transport of surface waters from the shelf towards the interior of the Ría. Flow cytometry analyses revealed an increase in the abundance of *Synechococcus* and, unexpectedly, the presence of *Prochlorococcus* (Cermeño et al., unpublished results). Although this group is characteristic of open ocean oligotrophic environments, several authors have pointed out its occurrence in coastal waters of the NW Iberian Peninsula, associated with the poleward Portugal coastal counter current (Calvo-Díaz et al., 2004). In addition to this, previous studies in the coastal transition zone of the Iberian upwelling system and the Southern Bay of Biscay have used taxonomic criteria such as the dominance of dinoflagellates and small flagellates or the absence of diatoms as indicators of shelf water intrusions (Fernández et al., 1991; Castro et al., 1997). The co-occurrence of *Synechococcus* and *Prochlorococcus*, as well as the increase in the relative contribution of picophytoplankton to total Chl *a* and POC-pr, suggest that advective processes, under strong downwelling conditions, may play a significant role in the ecological and biogeochemical functioning of this system.

However, other factors may also control phytoplankton size structure during the downwelling season. Low daily average irradiance and continuous vertical mixing may affect significantly phytoplankton size structure. Recent works suggest that under light-limited conditions, larger phytoplankton may be at a disadvantage over smaller cells, as the increase in intracellular chlorophyll *a* concentration cannot be compensated by a reciprocal increase in the light absorption, thus causing the 'package effect'. The package effect affects larger cells more strongly since their low surface-to-volume ratio limits an increase in the optical absorption cross section, which gives rise to a decrease in photosynthetic activity of larger phytoplankton (Finkel et al., 2004).

Thus, shelf water intrusions from oligotrophic, stratified environments, the high dispersal rates of phytoplankton under turbulent mixing conditions, and low daily average irradiances, are the main factors responsible for the low phytoplankton biomass and POC-pr rates measured during this period. Furthermore, it is likely that size-dependent limitation in light acquisition, suffered in a higher degree by larger phytoplankton (e.g. Finkel et al., 2004), accounts, to a great extent, for the reduced contribution of microphytoplankton to total biomass and primary production during the downwelling season.

4.4. Production and biomass of small and large phytoplankton

The higher contribution of large phytoplankton to total POC-pr than to total biomass ($P_L/P_T > B_L/B_T$) can be interpreted at two different, non-exclusive levels. First, it implies a preferential removal of larger phytoplankton due to grazing and sinking. Secondly, it suggests that large-sized phytoplankton have higher photosynthetic efficiencies than smaller cells.

Higher P_L/P_T than B_L/B_T implies that larger phytoplankton are preferentially exported from the ecosystem. Trophic coupling between large phytoplankton and mesozooplankton and higher sinking rates of large-sized phytoplankton and aggregates are implied in the size-differential export rates of phytoplankton assemblages (Legendre and Rassoulzadegan, 1996). In our study, preferential export of larger cells agrees with the conceptual models that predict a higher export of biogenic carbon in ecosystems dominated by large-sized phytoplankton assemblages, where the classical, short food chain prevails.

The size-fractionated, photosynthesis to Chl *a* ratios also suggests that, under favourable conditions for growth, namely high irradiance and nutrient concentration, large-sized phytoplankton may be more efficient than smaller cells in C assimilation. In principle, it is expected that small-sized cells are at an advantage over larger phytoplankton in nutrient acquisition and light absorption, owing to their higher surface-to-volume ratio (Kiørboe, 1993). However, taxon-related differences might override the size dependence of phytoplankton metabolism (Chisholm, 1992). For example, it is well known that for the same cell size, diatoms have higher photosynthetic efficiencies than dinoflagellates (Banse, 1982). Typically, phytoplankton growth rate responds to the intracellular quota of nutrients which may be increased by recent uptake or supplemented from stored reserves in vacuoles (Raven, 1997). Several studies have described how nutrient uptake rates frequently exceed the requirements imposed by cellular metabolic demands. This physiological mechanism, known as luxury uptake, is typically associated with vacuolated diatoms growing under intermittent upwelling conditions. As a result, this adaptive ability has been proposed as an ecophysiological strategy for large-sized cells under intermittent upwelling conditions (Geider et al., 1986). Moreover, recent work suggests that under favourable conditions for growth, larger cells, in particular diatoms, may have a higher photosynthetic efficiency due to an enhanced photochemical efficiency of photosystem II (Cermeño et al., 2005b).

4.5. Carbon budget and phytoplankton size structure

Phytoplankton size structure plays a major role in the carbon budget of microbial pelagic communities (Legendre and Le Fèvre, 1989). Theoretical models relate the export potential of pelagic ecosystems to their trophic structure. Typically, small-sized phytoplankton (<5 μm) form the basis of the microbial food web, characterized by the recycling of organic matter within the ecosystem. In contrast, large phytoplankton

(>5 μm) sustain the classical food chain, which favours the export of organic matter either to adjacent systems or to upper trophic levels. However, these contrasting situations represent only the ends of a continuum characterized by a more complex functioning, where carbon flows through the multivorous food web with continuous departures to the classical food chain and the microbial food web (Legendre and Rassoulzadegan, 1996).

The pelagic ecosystem of the Ría de Vigo showed two major patterns in phytoplankton size structure, corresponding to the upwelling and downwelling favourable seasons. During the upwelling favourable season, the increase in the relative contribution of large-sized phytoplankton to total biomass and production is likely to enhance the carbon flow through the classical, short food chain. This suggests a higher potential ability to export recently photosynthesised POC to higher trophic levels and adjacent ecosystems. During intense upwelling events, only a small fraction of the newly produced biomass is respired within the Ría, and most of it is likely to be exported by intense offshore circulation of surface waters (Álvarez-Salgado et al., 1996). In contrast, upwelling relaxation and stratification conditions give rise to an important accumulation and consumption of phytoplankton biomass, which concentrates typically in the subsurface chlorophyll maximum. However, as aforementioned, subsequent enhancement of offshore Ekman transport is likely accompanied by the export of large amounts of recently photosynthesised biogenic carbon from the Ría to the adjacent shelf and ultimately to the open ocean through offshore upwelling filaments (Joint et al., 2001). During the downwelling favourable season, an increase in the relative importance of pico- and small nanophytoplankton to total standing stocks and primary production is likely to reduce the potential ability of the ecosystem to export organic matter, thus enhancing recycling processes through the microbial food web. During this period, most of the recently photosynthesised organic carbon is remineralised within the microbial community.

In summary, a background level of pico- and small nanophytoplankton biomass and production, as well as the continuous production of dissolved organic carbon by the whole phytoplankton assemblage, were likely to maintain a considerable flow of matter through the microbial food web throughout the annual cycle. However, an increase in the relative contribution of large phytoplankton during favourable conditions for growth gives rise to an enhancement of the ecosystem's ability to export organic matter to the sediment and to adjacent areas, as well as to sustain upper trophic levels. Although the microbial plankton community of the Ría de Vigo exhibits a net autotrophic functioning throughout the year, there is an important degree of variability in the net community production, which seems to be dependent on phytoplankton size structure.

Acknowledgements

References

Agawin, N.S.R., Duarte, C.M., Agustí, S., 2000. Nutrient and temperature control of the contribution of picoplankton to phytoplankton biomass and production. Limnology and Oceanography 45, 591–600.

Álvarez, M., Fernández, E., Pérez, F.F., 1999. Air–sea CO_2 fluxes in a coastal embayment affected by upwelling: physical vs. biological control. Oceanologica Acta 22, 1–17.

Álvarez-Salgado, X.A., Gago, J., Míguez, B.M., Pérez, F.F., 2001. Net ecosystem production of dissolved organic carbon in a coastal upwelling system: the Ría de Vigo, Iberian Margin of the North Atlantic. Limnology and Oceanography 46, 35–147.

Álvarez-Salgado, X.A., Rosón, G., Pérez, F.F., Figueiras, F.G., Pazos, Y., 1993. Hydrographic variability off the Rías Baixas (NW Spain) during the upwelling season. Journal of Geophysical Research 98, 14447–14455.

Álvarez-Salgado, X.A., Rosón, G., Pérez, F.F., Figueiras, F.G., Pazos, Y., 1996. Nitrogen cycling in an estuarine upwelling system, the Ría de Arousa (NW Spain). II. Spatial differences in the short-time-scale evolution of fluxes and net budgets. Marine Ecology Progress Series 135, 259–273.

Banse, K., 1982. Cell volumes, maximum growth rates of unicellular algae and ciliates, the role of ciliates in the marine pelagial. Limnology and Oceanography 27, 1059–1071.

Banse, K., 1992. Grazing, temporal changes of phytoplankton concentrations, and the microbial loop in the open sea. In: Falkowski, P.G., Woodhead, A.D. (Eds.), Primary Productivity and Biogeochemical Cycles in the Sea. Plenum, New York, pp. 409–440.

Blanton, J.O., Atkinson, L.P., Castillejo, F.F., Montero, A.L., 1987. Coastal upwelling off the Rías Bajas, Galicia, Northwest Spain I: hydrographic studies. Rappapourt P-v Reunion Conseil International Exploration Mer 183, 79–90.

Calvo-Díaz, A., Morán, X.A.G., Nogueira, E., Bode, A., Varela, M., 2004. Picoplankton community structure along the northern Iberian continental margin in late winter–early spring. Journal of Plankton Research 26, 1069–1081.

Castro, C.G., Álvarez-Salgado, X.A., Figueiras, F.G., Pérez, F.F., Fraga, F., 1997. Transient hydrographic and chemical conditions affecting microplankton populations in the coastal transition zone of the Iberian upwelling system (NW Spain) in September 1986. Journal of Marine Research 55, 321–352.

Cermeño, P., Marañón, E., Rodríguez, J., Fernández, E., 2005a. Large-sized phytoplankton sustain higher carbon-specific photosynthesis than smaller cells in a coastal eutrophic ecosystem. Marine Ecology Progress Series 297, 51–60.

Cermeño, P., Estévez-Blanco, P., Marañón, E., Fernández, E., 2005b. Maximum photosynthetic efficiency of size-fractionated phytoplankton assessed by ^{14}C-uptake and fast repetition rate fluorometry. Limnology and Oceanography 50, 1438–1446.

Chisholm, S.W., 1992. Phytoplankton size. In: Falkowski, P.G., Woodhead, A.D. (Eds.), Primary Productivity and Biogeochemical Cycles in the Sea. Plenum, New York, pp. 213–237.

Fernández, E., Bode, A., Botas, A., Anadón, R., 1991. Microplankton assemblages associated with saline fronts during a spring bloom in the central Cantabrian Sea: differences in trophic structure between water bodies. Journal of Plankton Research 13, 1239–1256.

Figueiras, F.G., Niell, F.X., 1987. Composición del fitoplancton de la ría de Pontevedra (NO de España). Investigaciones Pesqueras 51, 371–409.

Figueiras, F.G., Pazos, Y., 1991. Microplankton assemblages in three Rías Baixas (Vigo, Arosa and Muros, Spain) with subsurface chlorophyll maximum: their relationships to hydrography. Marine Ecology Progress Series 76, 219–233.

Figueiras, F.G., Ríos, A.F., 1993. Phytoplankton succession, red tides and the hydrographic regime in the Rías Bajas of Galicia. In: Smayda, T.J., Shimizu, Y. (Eds.), Toxic Phytoplankton Blooms in the Sea. Elsevier Science Publishers BV, New York, pp. 239−244.

Finkel, Z.V., Irwin, A.J., Schofield, O., 2004. Resource limitation alters the 3/4 size scaling of metabolic rates in phytoplankton. Marine Ecology Progress Series 273, 269−279.

Fraga, F., 1976. Fotosíntesis en la Ría de Vigo. Investigaciones Pesqueras 40, 151−167.

Fraga, F., 1981. Upwelling of the Galician coast, Northwest Spain. In: Richards, F.A. (Ed.), Coastal Upwelling. American Geophysical Union, pp. 176−182.

Geider, R., Platt, T., Raven, J.A., 1986. Size dependence of growth and photosynthesis in diatoms: a synthesis. Marine Ecology Progress Series 30, 93−104.

Grasshoff, K., 1976. Methods of Seawater Analysis. Verlag Chemie, Weinheim, 317 pp.

Hansen, H.P., Grasshoff, K., 1983. Automated chemical analysis. In: Grasshoff, K., Ehrhardt, M., Kremling, K. (Eds.), Methods of Seawater Analysis. Verlag Chemie, Weinheim, pp. 347−395.

Hanson, R.B., Álvarez-Ossorio, M.T., Cal, R., Campos, M.J., Román, M., Santiago, G., Varela, M., Yoder, J.A., 1985. Plankton response following a spring upwelling event in the Ría de Arosa, Spain. Marine Ecology Progress Series 32, 101−113.

Joint, I., Inall, M., Torres, R., Figueiras, F.G., Álvarez-Salgado, X.A., Rees, A.P., Woodward, M.S., 2001. Two Lagrangian experiments in the Iberian Upwelling system: tracking an upwelling event and an off-shore filament. Progress Oceanography 51, 221−248.

Kiørboe, T., 1993. Turbulence, phytoplankton cell size and the structure of pelagic food webs. Advances in Marine Biology 29, 1−72.

Legendre, L., Le Fèvre, J., 1989. Hydrodynamical singularities as controls of recycled versus export production in oceans. In: Berger, W.H., Smetacek, V.S., Wefer, G. (Eds.), Productivity of the Oceans: Present and Past. John Wiley & Sons, pp. 49−63.

Legendre, L., Rassoulzadegan, F., 1996. Food-web mediated export of biogenic carbon in oceans: environmental control. Marine Ecology Progress Series 145, 179−193.

Malone, T.C., 1980. Algal size. In: Morris, I. (Ed.), The Physiological Ecology of Phytoplankton. Univ. California Press, Berkeley and Los Angeles, pp. 433−463.

Marañón, E., Cermeño, P., Fernández, E., Rodríguez, J., Zabala, L., 2004. Significance and mechanisms of photosynthetic production of dissolved organic carbon in a coastal eutrophic ecosystem. Limnology and Oceanography 49, 1652−1666.

Margalef, R., 1978. Life-forms of phytoplankton as survival alternatives in an unstable environment. Oceanologica Acta 1, 493−509.

Moncoiffé, G., Álvarez-Salgado, X.A., Figueiras, F.G., Savidge, G., 2000. Seasonal and short-time-scale dynamics of microplankton community production and respiration in an inshore upwelling system. Marine Ecology Progress Series 196, 111−126.

Mouriño, C., Fraga, F., 1985. Determinación de nitratos en agua de mar. Investigaciones Pesqueras 49, 81−96.

Nogueira, E., Pérez, F.F., Ríos, A.F., 1997. Seasonal patterns and long-term trends in an estuarine upwelling ecosystem (Ría de Vigo, NW Spain). Estuarine, Coastal and Shelf Science 44, 285−300.

Pérez, V., Fernández, E., Marañon, E., Serret, P., Varela, R., Bode, A., Varela, M., Varela, M.M., Morán, X.A.G., Woodward, E.M.S., Kitidis, V., García-Soto, C., 2005. Latitudinal distribution of microbial plankton abundance, production, and respiration in the Equatorial Atlantic in autumn 2000. Deep-Sea Research 52, 861−880.

Packard, T.T., 1979. Respiration and respiratory electron transport activity in plankton from the NW African upwelling area. Journal of Marine Research 37, 711−742.

Prego, R., 1993. General aspects of carbon biogeochemistry in the Ría de Vigo, northwestern Spain. Geochimica et Cosmochimica Acta 57, 2041−2052.

Quiñones, R.A., Platt, T., 1991. The relationship between the *f*-ratio and the P:R ratio in the pelagic ecosystem. Limnology and Oceanography 36, 211−213.

Raimbault, P., Rodier, M., Taupier-Letage, I., 1988. Size fraction of phytoplankton in the Ligurian Sea and the Algerian Basin (Mediterranean Sea): size distribution versus total concentration. Marine Microbial Food Webs 3, 1−7.

Raven, J.A., 1997. The vacuole: a cost-benefit analysis. Advances in Botanical Research 25, 59−86.

Riegman, R., Kuipers, B.R., Noordeloos, A.A.M., White, H.J., 1993. Size-differential control of phytoplankton and the structure of plankton communities. Netherlands Journal of Sea Research 31, 255−265.

Rodríguez, J., et al., 2001. Mesoscale vertical motion and the size structure of phytoplankton in the ocean. Nature 410, 360−363.

Serret, P., Robinson, C., Fernández, E., Teira, E., Tilstone, G., 2001. Latitudinal variation of the balance between plankton photosynthesis and respiration in the eastern Atlantic Ocean. Limnology and Oceanography 46, 1642−1652.

Smith, E.M., Kemp, W.M., 2001. Size structure and the production/respiration balance in a coastal plankton community. Limnology and Oceanography 46, 473−485.

Tamigneaux, E., Legendre, L., Klein, B., Mingelbier, M., 1999. Seasonal dynamics and potential fate of size-fractionated phytoplankton in a temperate nearshore environment (Western Gulf of St. Lawrence, Canada). Estuarine, Coastal and Shelf Science 48, 253−269.

Teira, E., Serret, P., Fernández, E., 2001. Phytoplankton size-structure, particulate and dissolved organic carbon production and oxygen fluxes through microbial communities in the NW Iberian coastal transition zone. Marine Ecology Progress Series 219, 65−83.

Tilstone, G.H., Figueiras, F.G., Fermin, E.G., Arbones, B., 1999. Significance of nanophytoplankton photosynthesis and primary production in a coastal upwelling system (Ría de Vigo, NW Spain). Marine Ecology Progress Series 183, 13−27.

Tilstone, G.H., Figueiras, F.G., Fraga, F., 1994. Upwelling−downwelling sequences in the generation of red tides in a coastal upwelling system. Marine Ecology Progress Series 112, 241−253.

Tilstone, G.H., Miguez, B.M., Figueiras, F.G., Fermín, E.G., 2000. Diatom dynamics in a coastal ecosystem affected by upwelling: coupling between species succession, circulation and biogeochemical processes. Marine Ecology Progress Series 205, 23−41.

Tremblay, J.-E., Klein, B., Legendre, L., Rivkin, R.B., Therriault, J.-C., 1997. Estimation of *f*-ratios in oceans based on phytoplankton size structure. Limnology and Oceanography 42, 595−601.

Tremblay, J.-E., Legendre, L., 1994. A model for the size-fractionated biomass and production of marine phytoplankton. Limnology and Oceanography 39, 2004−2014.

Wooster, W.S., Bakun, A., Maclain, D.R., 1976. The seasonal upwelling cycle along the eastern boundary of the North Atlantic. Journal of Marine Science 34, 131−141.